

# PROCEEDINGS REPRINT

 SPIE—The International Society for Optical Engineering

*Reprinted from*

## ***Optical Methods for Time- and State-Resolved Chemistry***

23–25 January 1992  
Los Angeles, California



**Volume 1638**

# Vibrational spectroscopy and picosecond dynamics of gaseous trienes and tetraenes in $S_1$ and $S_2$ electronic states

Hrvoje Petek, Andrew J. Bell, Ronald L. Christensen,\* and Keitaro Yoshihara

Institute for Molecular Science,  
Myodaiji, Okazaki 444 Japan  
and \*Department of Chemistry  
Bowdoin College  
Brunswick, Maine 04011

## ABSTRACT

Fluorescence excitation and emission spectra of the  $S_1$  and  $S_2$  states of model trienes and tetraenes are measured in free jet expansions. The barriers to *cis-trans* isomerization in the  $S_1$  state are  $<200\text{ cm}^{-1}$  for trienes and  $\sim 2000\text{ cm}^{-1}$  for tetraenes.  $<250\text{ fs}$  nonradiative decay of the  $S_2$  state of tetraenes is deduced from the observed Lorentzian linewidths.

## 1 INTRODUCTION

Nature has harnessed polyenes as transducers for converting light into chemical energy by exploiting their ability to undergo photochemical *cis-trans* isomerization.<sup>1,2</sup> Thus polyenes can be found to perform vital functions in processes such as vision and plant and bacterial photosynthesis. Furthermore, their unique electronic structure makes polyenes attractive for potential applications as organic conductors and nonlinear optical materials with large third-order susceptibilities.<sup>3</sup> There is a growing effort to exploit the unique electronic structure and reactivity of polyenes as chemical sensors, switches, logic devices, etc. In order to incorporate polyenes into useful functional devices it is imperative to understand such fundamental properties as the dependence of the electronic structure on the conjugation length and the effect of substitution on the structure and reactivity of the chromophore.<sup>1</sup> Most of the interesting photochemical transformations occur in the three low energy electronic states - the  $1^1A_g$  ground state ( $S_0$ ),  $2^1A_g$  first excited state ( $S_1$ ), and  $1^1B_u$  second excited state ( $S_2$ ). Since the  $S_2 \leftarrow S_0$  transition is strongly allowed, the  $S_2$  state is the chromophore in simple polyene systems. Because the  $S_1 \leftarrow S_0$  ( $2^1A_g \leftarrow 1^1A_g$ ) transition is forbidden by symmetry, it is usually produced by  $S_2 \leftarrow S_0$  excitation followed by subpicosecond timescale  $S_2 \rightarrow S_1$  internal conversion. Since both the  $S_1$  and  $S_2$  states play important roles in the biological activity of polyenes, we have made a systematic study of the electronic structure and dynamics of the  $S_1$  and  $S_2$  states of short linear polyenes (trienes<sup>4</sup> and tetraenes<sup>5</sup>) under molecular beam conditions and in solution phase.

## 2. EXPERIMENTAL

The experimental setup used to measure fluorescence excitation spectra under collision free conditions have been described.<sup>5</sup> The apparatus consists of; (i) a vacuum chamber together with a pulsed valve, for production of the molecular beam; (ii) an excimer pumped dye laser for excitation of the molecule under study; and (iii) emission collection optics and electronics.

*All-trans*-2,4,6,8-decatetraene (DT), *all-trans*-2,4,6,8-nonatetraene (NT), and octatriene were prepared respectively from the Wittig reaction between hexadienal (Aldrich) and crotyltriphenylphosphonium bromide, allyltriphenylphosphonium bromide, and ethyltriphenylphosphonium bromide (Fluka), as described previously.<sup>6</sup> The samples were purified by column chromatography followed by recrystallization in hexane for tetraenes. This procedure was sufficient to get  $>95\%$  pure *all-trans*-

tetraenes. The analysis of octatriene by GC/MS and HPLC showed it to contain >90% *all-trans*-octatriene together with small amounts of *cis*-isomers. The hexatriene sample, consisting of a mixture of isomers, was obtained from Aldrich Chemical Company (cat. no.# H1,258-7) and used as obtained without separating the isomers. The samples were introduced into the vacuum chamber through the 500  $\mu\text{m}$  orifice of the pulsed valve. Tetraene samples were heated to 40 - 70° C, and triene samples were used at room temperature. The samples were coexpanded with He carrier gas at a total pressure of 100 - 3000 Torr. Pressures of <300 Torr were used in the  $S_2 \leftarrow S_0$  fluorescence excitation measurements because the spectra were sensitive to the presence of clusters at higher pressures.

The excitation source consisted of an excimer pumped dye laser system (Lambda-Physik 104/2003). The bandwidth of the laser was  $\sim 0.3 \text{ cm}^{-1}$ , with a pulsewidth of  $\sim 15 \text{ ns}$ . The experiment was performed with a laser repetition rate of 10 Hz and the dye laser wavelength was calibrated by measuring the optogalvanic spectrum of neon using a neon filled hollow cathode lamp. The laser beam intersected the molecular beam 15 mm from the nozzle orifice. At this distance the polyenes were found to be collision free, on the time scale of the experiment. The laser intensity was carefully adjusted to optimize the signal while avoiding saturation of the transitions. Fluorescence was collected by a single f/1 quartz lens and detected by a photomultiplier tube (Hamamatsu Photonics H3177). The signal was captured with a gated integrator (SRS 250) and then passed to a microcomputer along with a monitor of the dye laser intensity for normalization. For the measurement of lifetimes the fluorescence decay signal was digitized and averaged using a digital storage oscilloscope (Le Croy 7400A) and transferred to a microcomputer for analysis by fitting to a single exponential decay profile.

### 3. $S_1$ STATE SPECTRA OF TRIENES

The fluorescence excitation spectrum measured with a mixture of *cis*- and *trans*-hexatrienes is shown in Fig. 1. The positions and relative intensities of the peaks are given within the figure. Based on the assignment of previously measured Resonance Enhanced Multiphoton Ionization (REMPI) spectrum by Buma *et al.*,<sup>7</sup> the spectrum in Fig. 1 is assigned to the  $S_1$  state of the *cis*-hexatriene. Even though the concentration of the *trans*-isomer is at least as great as the *cis*-isomer, its spectrum could not be observed. The origin region consists of two major peaks separated by  $\sim 5.7 \text{ cm}^{-1}$ . This doublet shows further structure due to partially resolved rotational features. Changing the expansion conditions affects the rotational structure, however, the relative integrated intensities of the two bands are not changed. The rotational lineshapes of the origin bands are consistent with a predominantly parallel transition of *cis*-hexatriene. The  ${}^1A_1 \leftarrow {}^1A_1$  transition is allowed for a molecule with a  $C_{2v}$  symmetry, however, a perpendicular band is expected. This spectrum appears to derive its oscillator strength by intensity borrowing from the  $S_2 \leftarrow S_0$  transition. This is a common feature to all linear polyene spectra presented here: the symmetry forbidden  $2{}^1A_g \leftarrow 1{}^1A_g$  transition gains intensity by vibronic coupling between  $1{}^1B_u$  and  $2{}^1A_g$  states. Although the presence of a *cis*-linkage or asymmetric substitution by a methyl group breaks the molecular symmetry, the dominant effect which determines the oscillator strength for the  $S_1 \leftarrow S_0$  spectra of linear polyenes is vibronic coupling. For that reason g and u symmetry labels will be retained throughout this text, even though the labels may not apply strictly to individual molecules.

The ratio of the fluorescence excitation spectrum intensity relative to the REMPI spectrum drops rapidly between the peaks at 71.3 and 157.7  $\text{cm}^{-1}$ . Since the hexatriene lifetimes are shorter than the experimental time resolution, these intensity ratios provide indirect evidence for a nonradiative decay channel with an activation energy between 71.3 and 157.7  $\text{cm}^{-1}$ , as will be explained below. Due to a rapid decrease in the fluorescence quantum yields, the highest energy peaks which could be detected are at 247 - 263  $\text{cm}^{-1}$  (not shown), however, the REMPI spectrum is seen to increase in intensity for >4000  $\text{cm}^{-1}$  above the origin.

The fluorescence excitation spectrum of octatriene, and the fluorescence lifetimes measured at several peaks are shown in Fig. 2. Qualitatively, the fluorescence excitation spectrum is similar to a previously measured REMPI spectrum of a *cis*-octatriene isomer.<sup>8</sup> The smaller fluorescence yields of other isomers that are present in the sample, such as *all-trans*-octatriene which comprises ~90% of the sample, precludes their detection in our experiments. The origin, which could not be determined with certainty in the REMPI study is found to be at 33648 cm<sup>-1</sup>. As in *cis*-hexatriene, there are considerable differences between the fluorescence excitation and REMPI spectra at high excess energy, where the fluorescence excitation spectrum rapidly drops in intensity to below the detection limit, while the REMPI spectrum has further vibrational structure followed by a rising continuous absorption.<sup>8</sup> Since *cis*-octatriene isomers could not be isolated in either REMPI or the present study, the true structure of the octatriene responsible for the spectrum in Fig. 2 has not yet been determined.<sup>4,8</sup>

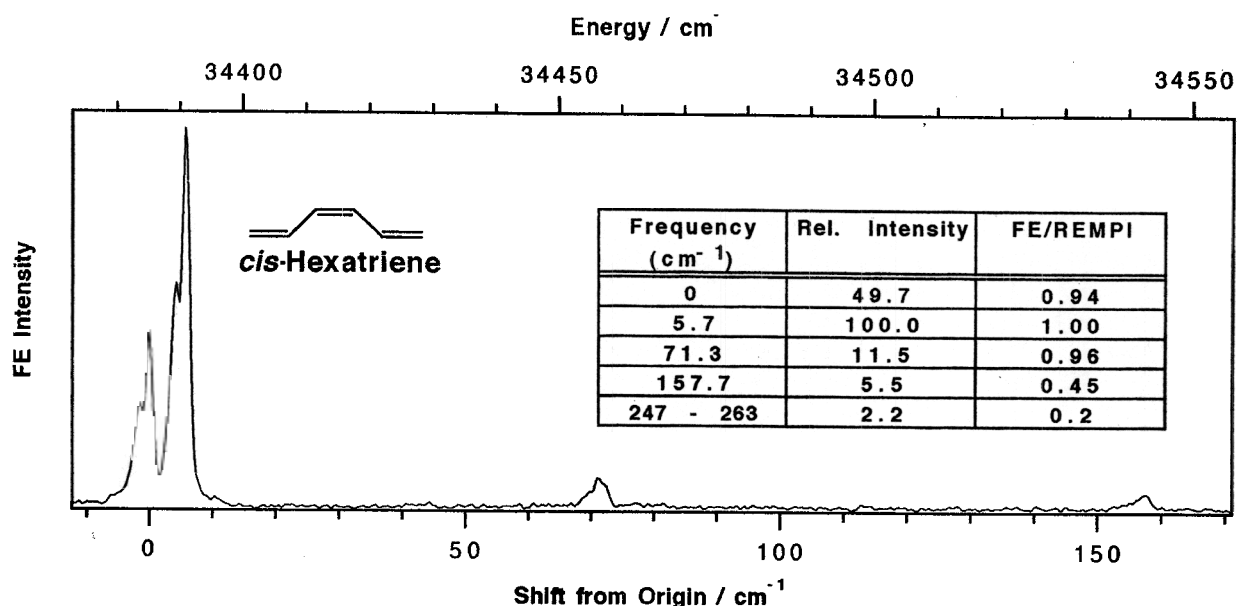


**Figure 1.** The fluorescence excitation spectrum of hexatriene. The abscissa shows both absolute energy and energy shift from the origin. The molecular beam was formed by coexpanding hexatriene with helium at a pressure of 575 Torr. The origin is at 34382 cm<sup>-1</sup>. The table gives the ratios of integrated intensities for individual peaks measured by REMPI<sup>7</sup> and fluorescence excitation.

The octatriene fluorescence lifetimes measured for states with <200 cm<sup>-1</sup> excess energy show a reproducible scatter about an average of 63 ns. This may be due to the vibrational dependence of radiative and nonradiative decay rates, or possibly due to the presence of two or more octatriene isomers. The marked decrease in the fluorescence lifetimes shown in Fig. 2 coincides with the drop in fluorescence excitation spectral intensity relative to the REMPI spectrum.<sup>8</sup> This implies a sudden decrease in the fluorescence quantum yields as is also observed in hexatriene at low excess energies.

Even though the S<sub>1</sub> states of hexatriene and octatriene have similar electronic structures, their spectra are remarkably different. The hexatriene spectrum is simpler, but the splitting of most lines, including the origin, into two or more peaks, indicates that the S<sub>1</sub> state surface has some complex features. Buma *et al.* made a proposal supported by *ab initio* calculations that this splitting is due to out-of-plane distortion of the terminal hydrogens which gives rise to two distinct geometries in the S<sub>1</sub> state.<sup>7</sup> The presence of the methyl groups make the spectrum of octatriene significantly more complex than that

of hexatriene. The phenomenally large number of lines observed in the first 250  $\text{cm}^{-1}$  of the octatriene spectrum implies a large geometrical change upon  $S_1 \leftarrow S_0$  excitation, most likely torsion of the methyl groups. In addition, torsion of the CC bonds and out-of-plane bending distortions of methyl groups, that are analogous to the hydrogen bending proposed for hexatriene, also may contribute.<sup>4</sup>

The 15 ns upper limit for the *cis*-hexatriene  $S_1$  state lifetime is considerably shorter than the  $\sim 350$  ns decays observed for isolated *all-trans*-decatetraene<sup>5</sup> and *all-trans*-nonatetraene (*vide infra*). This indicates that, even at the origin, the fluorescence quantum yield of hexatriene is significantly less than unity. Relative lifetimes as a function of vibronic energy can be deduced from the comparison between relative integrated peak intensities observed in fluorescence excitation and REMPI spectra tabulated in Fig. 1. The intensity of lines in the REMPI spectra mainly are dictated by the absorption of the species (assuming that the ionization rate is faster than the nonradiative decay rate and that the  $S_1 \leftarrow S_0$  transition is not saturated), whereas the fluorescence excitation spectra are controlled by the product of the absorption cross section and fluorescence quantum yield.<sup>4,7</sup> The decrease of the intensity ratios from unity above 71.3  $\text{cm}^{-1}$  starting with the peak at 157.7  $\text{cm}^{-1}$ , implies that a nonradiative decay channel opens up in this energy interval. Thus in hexatriene there are at least two processes which lead to nonradiative decay: one appears to be energy independent, and the other has an activation energy of  $< 157.7$   $\text{cm}^{-1}$ . Further evidence for a low barrier on the  $S_1$  state surface may be the continuous absorption in the REMPI spectrum. This continuum may be due to a rapid increase in the density of vibrational states due to the anharmonicity of the  $S_1$  state surface, or due to the coupling between the  $S_1$  and another dark state.<sup>4</sup>

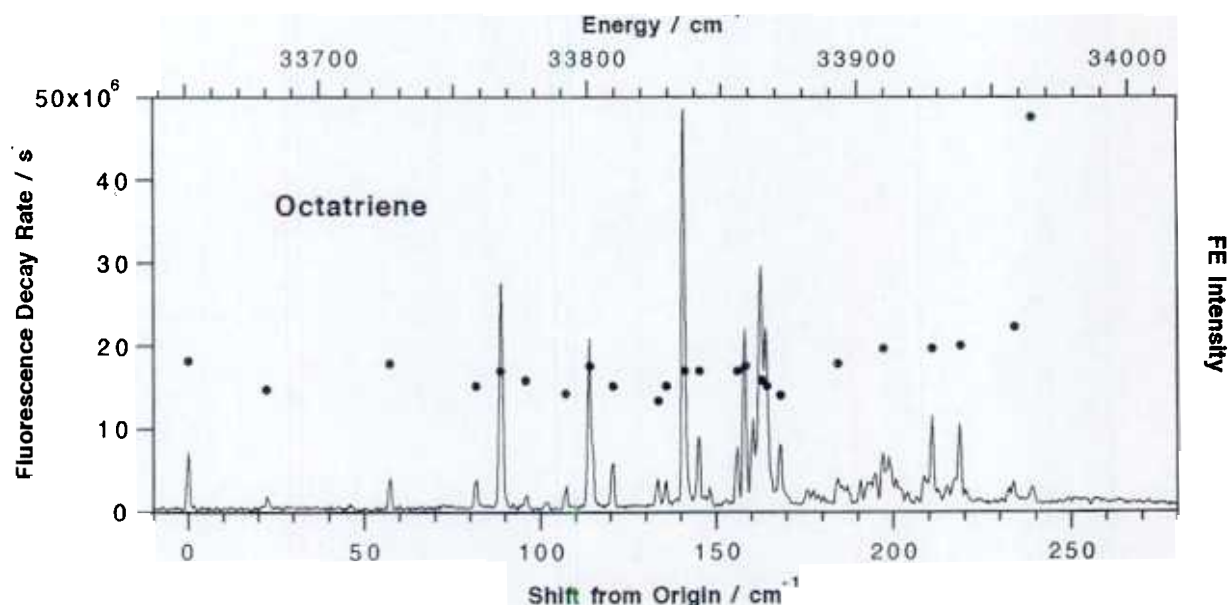


**Figure 2.** The fluorescence excitation spectrum of octatriene. The abscissa shows both absolute energy and energy shift from the origin. The ordinate shows the fluorescence decay rate (left) and fluorescence excitation intensity (right). Also shown are lifetimes for the major peaks. The error bars correspond to one standard deviation determined from the fit of the fluorescence decays to single exponentials. The origin is at 33648  $\text{cm}^{-1}$ .

Although the octatriene lifetimes are significantly longer than those of hexatriene, their shortness (relative to the tetraenes)<sup>6</sup> and the variation in lifetimes in the  $<200\text{ cm}^{-1}$  energy region may be due to nonradiative decay processes that have a weak dependence on energy and quantum state. The decrease in octatriene lifetimes and the loss of the fluorescence excitation spectrum intensity above  $200\text{ cm}^{-1}$  from the origin both are indicative of nonradiative decay by barrier crossing. The transition from discrete vibrational structure to the continuous absorption seen in the REMPI spectrum at higher energies probably implies an abrupt increase in the density of states above the barrier. As in hexatriene, there is evidence for two distinct nonradiative decay mechanisms.<sup>4</sup>

#### 4. FLUORESCENCE EXCITATION SPECTRA OF TETRAENES

The fluorescence excitation spectra of DT and NT are measured from their  $S_1 \leftarrow S_0$  origins at  $\sim 345\text{ nm}$  to  $265\text{ nm}$ . The spectra of both molecules show the presence of two electronic states of greatly different character. The  $S_2$  state with origins at  $\sim 287.47\text{ nm}$  ( $34786\text{ cm}^{-1}$ ) for DT and  $284.97\text{ nm}$  ( $35091\text{ cm}^{-1}$ ) for NT, corresponds to the intense near uv-visible  $\pi^* \leftarrow \pi$  transition seen in the solution phase absorption spectra of polyenes.<sup>1</sup> Previously, we have shown that the excitation of tetraenes to the  $S_2$  state under collision free conditions results in emission from both  $S_1$  and  $S_2$  states.<sup>5,6</sup> Below the  $S_2$  state, there is a considerably weaker  $S_1 \leftarrow S_0$  spectrum, which can only be seen in emission from intermediate length polyenes in solution. Under supersonic expansion conditions the  $S_1 \leftarrow S_0$  fluorescence excitation spectra of DT and NT are characterized by sharp vibrational structures, a complex vibrational developments, and maxima in intensity at the C = C stretching fundamentals, which are at  $\sim 1793\text{ cm}^{-1}$  above the origins. Above the C = C stretch the sharp structure gradually is replaced by a broad continuum.

##### 4.1 $S_1 \leftarrow S_0$ Fluorescence Excitation Spectra

**Decatetraene.** The measured fluorescence excitation spectra of the  $S_1 \leftarrow S_0$  transition and the fluorescence decay rates for DT are shown in Fig. 3a. The origin of the DT  $S_1 \leftarrow S_0$  spectrum has been assigned to the intense triplet of peaks with the center of the lowest energy feature at  $29022\text{ cm}^{-1}$ .<sup>5</sup> Since the  $2^1A_g \leftarrow 1^1A_g$  transition is strictly forbidden by symmetry, this is probably a false origin, as will be discussed further. In Fig. 3 it can be seen that the low energy region is rather complicated due to excitation of many low frequency modes which involve skeletal bending vibrations and methyl torsions. Many low frequency modes derive intensity from Herzberg-Teller coupling between the  $2^1A_g$  and  $1^1B_u$  states, which makes the  $2^1A_g \leftarrow 1^1A_g$  symmetry forbidden transition vibronically allowed.<sup>1,5</sup> There are at least two types of low frequency  $b_u$  symmetry modes, methyl torsion and in-plane bending, which break the molecular symmetry and make the spectrum weakly allowed. The characteristic signature of methyl torsion induced transitions is a triplet structure with a  $3.4\text{ cm}^{-1}$  splitting (doublet in case of nonatetraene, which has only one methyl); for the transitions which are induced by  $b_u$  symmetry in-plane bending the signature is a singlet structure. High resolution fluorescence excitation spectra of DT and NT  $S_1 \leftarrow S_0$  origin regions are shown in Fig. 4. The  $\sim 3.4\text{ cm}^{-1}$  splitting is due to the tunneling of two equivalent methyl groups through a low barrier on the  $S_1$  state surface. Assuming that the surface for methyl torsion is given by a simple sinusoidal potential and that the two methyl groups are not coupled, a barrier of  $\sim 40\text{ cm}^{-1}$  reproduces the observed splitting and it also successfully predicts the line positions of a number of observed low frequency lines in both DT and NT, which are due to excitation of higher quanta of methyl torsion.<sup>9</sup>

At higher energies we can identify two prominent features, the C - C stretch at  $1231\text{ cm}^{-1}$  and C = C stretch at  $1793\text{ cm}^{-1}$ . The CC stretches have the largest Franck-Condon factors due to the well known bond order inversion between the  $S_1$  and  $S_0$  states, which is common to all linear polyenes.<sup>1</sup> The

frequencies of CC stretches in the  $S_1$  states of symmetric (or nearly symmetric) polyenes are unusually high. This is characteristic of the  $S_1$  states of polyenes, and can be ascribed to strong vibronic coupling between the  $S_1$  and  $S_0$  states.<sup>10</sup>

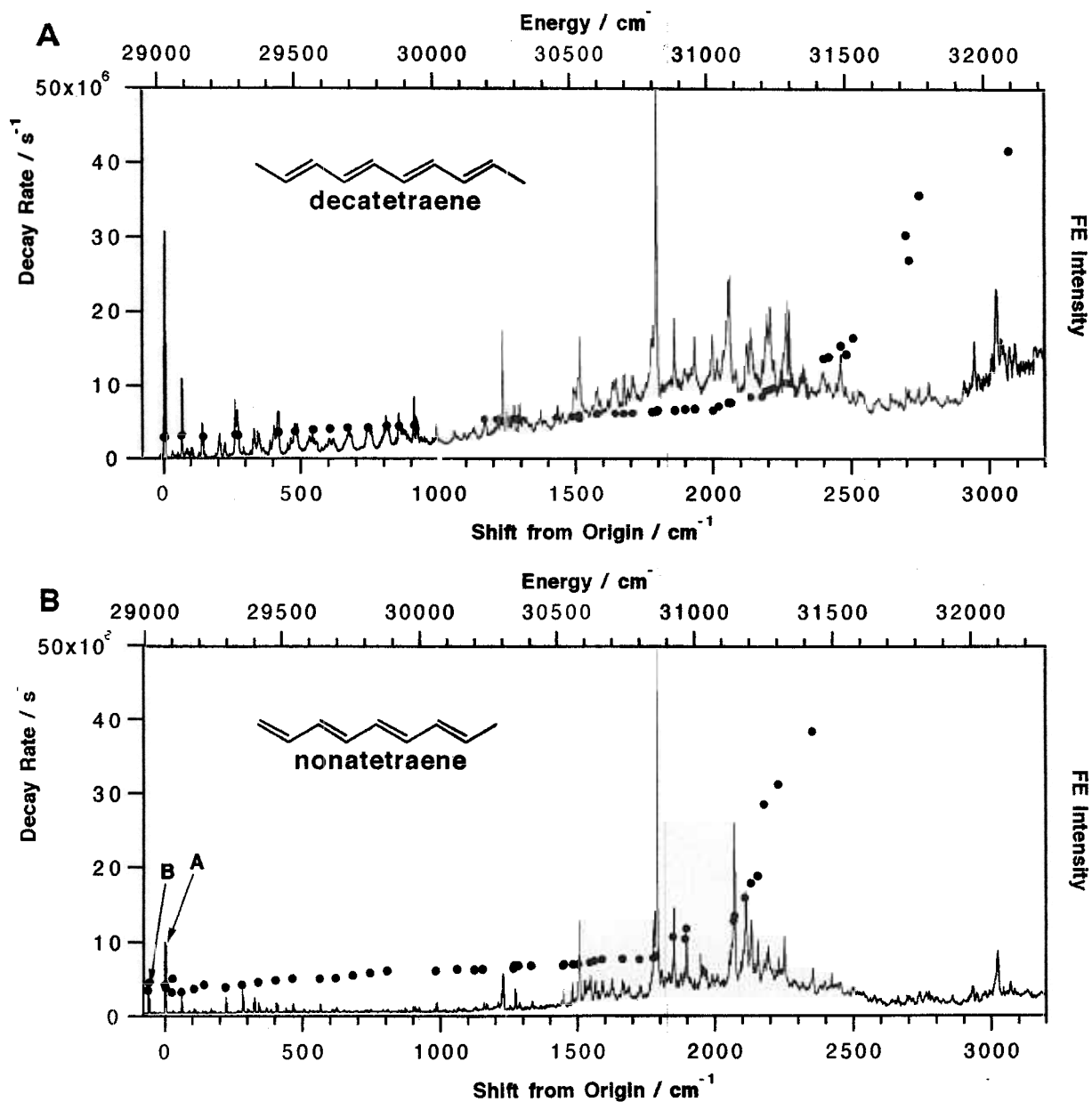


**Figure 3.** The  $S_1 \leftarrow S_0$  fluorescence excitation spectra and single vibronic level fluorescence decay rates ( $\bullet$ ) of DT (a) and NT (b). The two origins seen in the NT spectrum are indicated by "A" and "B". The most intense feature in both spectra is assigned to the C = C stretch fundamental. The discontinuous change in the decay rates at  $\sim 2000 \text{ cm}^{-1}$  excess energy is due to onset of nonradiative decay as described in the text.

The commonly observed increase in intensity in the  $2^1A_g \leftarrow 1^1A_g$  absorption spectra of polyenes in solutions with increase in energy can be attributed to two causes: i) the vibronic coupling between the  $2^1A_g$  and  $1^1B_u$  states; and ii) the Franck-Condon factors for the C - C and C = C stretching vibrations.<sup>1</sup> The increase in vibronic coupling with excess energy due to a decrease in the energy gap between the  $2^1A_g$  and  $1^1B_u$  states is responsible for the modest increase in the absorption and emission rates for states with  $<2000 \text{ cm}^{-1}$  excess energy seen in Fig 3. From the absorption spectra of octatetraene in solution<sup>11</sup> and emission spectra of DT and NT measured in this work (Fig. 5), we expect the maximum in the  $S_1 \leftarrow S_0$  absorption spectra of tetraenes to be at a considerably higher energy than the intensity maximum observed in the DT and NT fluorescence excitation spectra. The maximum in emission intensity upon exciting the origin of DT and NT occurs for a combination band with two quanta of C = C stretch and one quantum of C - C stretch at  $\sim 4,500 \text{ cm}^{-1}$  above the origin (Fig. 5). The Franck-Condon maximum is expected to be at an even higher energy in  $S_1 \leftarrow S_0$  absorption due to the steeper slope of the  $S_1$  state potential energy surface in the CC stretching coordinates as compared to the  $S_0$  state. In fact, *ab initio* and semi-empirical calculations predict that the vertical excitation from the ground state geometry is at a higher energy for the  $2^1A_g$  state than for the  $1^1B_u$  state.<sup>2</sup> The discrepancy between the expected and observed maxima in the  $S_1 \leftarrow S_0$  fluorescence excitation spectrum is due to a nonradiative decay process which has an activation energy of  $\sim 2000 \text{ cm}^{-1}$ . We will discuss this further in the context of lifetime measurements.

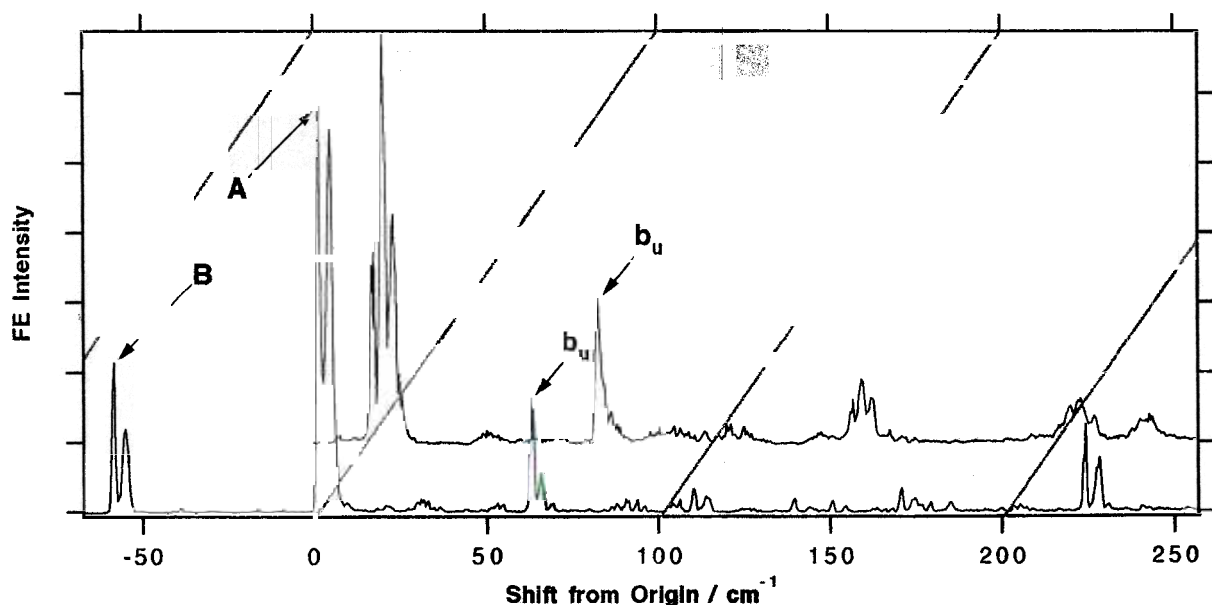


**Figure 4.** High resolution fluorescence excitation spectra of DT (top) and NT (bottom)  $S_1 \leftarrow S_0$  origins. The two origins observed in NT are indicated by "A" and "B". Most of the lines are split into triplets (DT) and doublets (NT) with a  $3.4 \text{ cm}^{-1}$  splitting due to the tunneling of the methyl groups. However, the  $b_u$  symmetry modes appear as singlets, for example the in-plane bending fundamentals indicated by " $b_u$ ".

**Nonatetraene** Although DT and NT have very similar structures, their  $S_1 \leftarrow S_0$  spectra exhibit large differences. Again the spectrum (Fig. 3b) consists of many low frequency modes due to methyl torsion and in-plane bending. However, the spectrum is much sharper at higher energies, because the density of vibrational states grows with energy more slowly than for DT.

The origin of the NT spectrum cannot be trivially assigned to the lowest energy feature. In the origin region (Fig. 3b and 4) there are two pairs of lines which might be assigned to the origin. Both pairs are split by  $\sim 3.4 \text{ cm}^{-1}$  due to the tunneling of a single methyl group. This splitting is an exquisitely sensitive probe of the electronic structure in the vicinity of the methyl group, so the fact that both pairs of lines show the same splitting, which is essentially the same as the splitting in DT, indicates that the methyl groups are experiencing very similar repulsive and attractive interactions.

The C = C stretching fundamental, which is expected to be the most intense peak by analogy with DT, is a useful guide for locating the origin. If the most intense line in the spectrum is assigned to the C = C stretching fundamental and the most intense line in the origin region at  $29072 \text{ cm}^{-1}$  (we will call it origin "A") is taken to be the origin, then the C = C stretching frequency is  $1793 \text{ cm}^{-1}$ , as in DT. However, origin A is not the lowest energy feature in the spectrum. The lowest energy feature at  $29012 \text{ cm}^{-1}$  (we will call it origin "B") has integrated intensity  $\sim 1/4$  as large as the origin A independent of the sample preparation, the temperature of the sample reservoir in the pulsed nozzle (which is also the same temperature as the nozzle), and the He stagnation pressure. However, the only line in the C = C stretching region which can be associated with the origin B has  $< 1/20$  of the intensity of the C = C stretch assigned to the origin A.

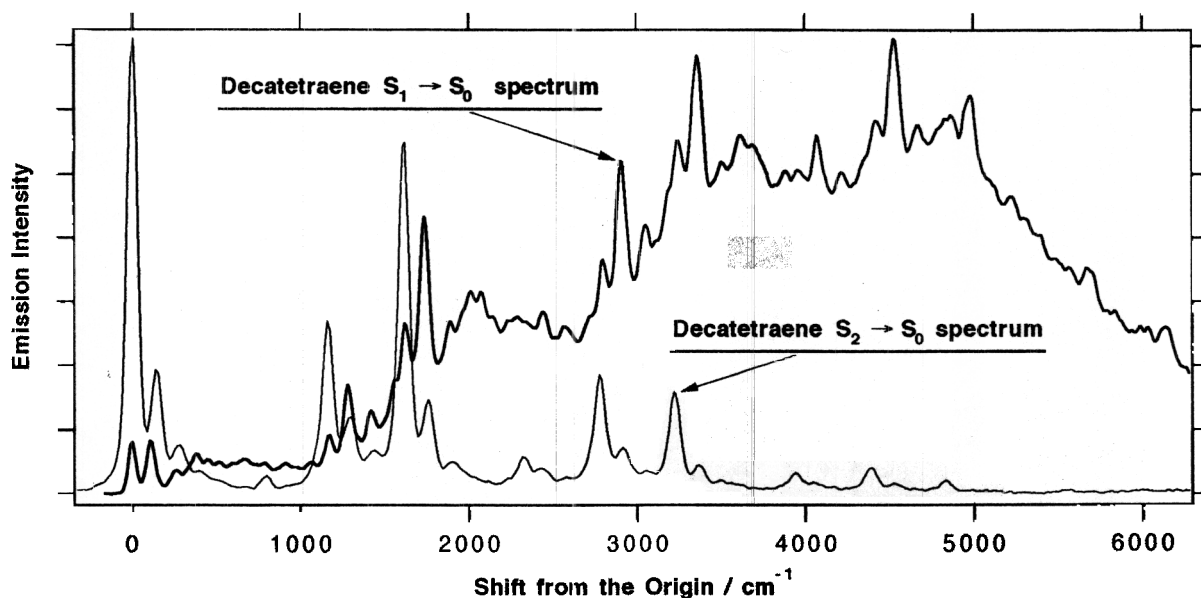


**Figure 5.** The emission spectra from the origins of  $S_1$  (thicker line) and  $S_2$  states. The very broad intensity distribution in the  $S_1 \rightarrow S_0$  spectrum is due to the bond order reversal for CC stretching in the  $S_1$  state. By contrast, the  $S_2$  state has much smaller displacement in CC stretching with respect to the  $S_0$  state.

Further information on the nature of origins A and B can be gained from the rotational bandshapes, emission lifetimes, and emission spectra. In the low excess energy region ( $< 350 \text{ cm}^{-1}$  above B) there appear to be two progressions with nearly identical frequency intervals but different lifetimes: the one associated with B has relatively longer lifetimes of 350 - 300 ns and narrower rotational bandshapes; the other, which is associated with A, has shorter lifetimes of 300 - 270 ns and broader rotational

bandshapes. The difference in the lifetimes and the rotational profiles suggests that these two sets of lines belong to molecules which have different molecular structures at least in the  $S_1$  state. However, the emission spectra from A and B show that the vibrational structure due to the C - C and C = C stretching vibrations in the  $S_0$  state is identical to within  $\pm 5 \text{ cm}^{-1}$  up to  $6000 \text{ cm}^{-1}$  excess vibrational energy. If the molecular structure were different for the species that give rise to A and B in the  $S_0$  state this would not be the case. For instance, a comprehensive study by Tasumi and co-workers of the  $S_0$  state vibrational spectra of hexatriene isomers and rotamers shows that the C - C stretching frequency is very sensitive to the molecular structure: the C - C stretching for *cis*-hexatriene is  $56 \text{ cm}^{-1}$  higher than for *trans*-hexatriene.<sup>12</sup> These observations point to the possibility that there are two nearly isoenergetic conformations on the  $S_1$  state surface of *all-trans*-nonatetraene, which can be accessed by optical excitation from the vibrationally and rotationally cold NT. Above  $350 \text{ cm}^{-1}$  excess energy in the  $S_1$  state the lifetimes do not show quantum state dependence suggesting that at these energies the two conformations are no longer distinct. At this energy the emission spectra are nearly structureless due to intramolecular vibrational redistribution (IVR) which is apparently faster than the emission rate. The IVR results in a loss of identity between A and B species. There is *no* evidence in the measured fluorescence lifetimes that the B species disappears above  $350 \text{ cm}^{-1}$  excess energy due to opening up of a nonradiative decay channel.

#### 4.2 $S_1$ state fluorescence decay measurements

The measured fluorescence decay rates as a function of excess energy for DT and NT are displayed in Fig. 3. For both DT and NT the fluorescence lifetimes are seen to decrease from  $\sim 350 \text{ ns}$  at the origin by approximately 1/2 upon increasing the excess energy to  $2000 \text{ cm}^{-1}$ . The increase of the radiative decay rate as a function of  $S_2 - S_1$  separation is commonly observed in the  $S_1$  states of polyenes in solution and is attributed to the intensity borrowing between  $S_2$  and  $S_1$  states.<sup>1</sup> For NT there is a large quantum state dependence in the decay rates in the low energy region, as discussed above.

Above  $2000 \text{ cm}^{-1}$  excess energy there is a rapid increase in the decay rates in both DT and NT. Such a discontinuous change in the decay rate is evidence for an energy activated nonradiative decay channel such as isomerization. As discussed above, the absorption maximum for  $S_1 \leftarrow S_0$  spectrum is implied to be  $>4500 \text{ cm}^{-1}$  above the origin by the large Stokes shift in the emission. This lack of mirror symmetry between fluorescence excitation and emission spectra above the C = C stretch fundamental is further evidence for nonradiative decay above  $2000 \text{ cm}^{-1}$  excess energy. Although there have been no measurements on *trans-cis* isomerization of DT and NT under isolated conditions or in solution, Kohler and coworkers have extensively studied *cis-trans* isomerization of several octatetraene isomers in low temperature mixed crystals.<sup>13</sup> Since isomerization of octatetraene is well established, we tentatively assign this nonradiative decay process to *cis-trans* isomerization. Since the IVR rate is much faster than the fluorescence decay rate at  $2000 \text{ cm}^{-1}$  excess energy, it is a good assumption that the energy is statistically distributed in all of the available vibrational degrees of freedom, and that the barrier to isomerization is located where the decay rate begins to increase rapidly. The faster fluorescence decay rate and greater loss of intensity in NT as compared with DT at comparable energies above the barrier is due to the lower density of states in NT.

### 5. $S_2$ STATE SPECTRA OF TETRAENES

The fluorescence excitation spectra of the  $S_2$  state of DT and NT are shown in Fig. 6. The spectra were found to be extremely sensitive to the excitation laser fluence and the expansion conditions. The laser was attenuated to the point where the fluorescence intensity had a linear dependence on the laser power. At low stagnation pressures ( $<200 \text{ Torr He}$ ) and low tetraene concentration, the emission decay was too fast to resolve with the instrumental time resolution of  $\sim 15 \text{ ns}$ . At higher He stagnation pressures and tetraene concentrations there was an additional long lived decay component and several

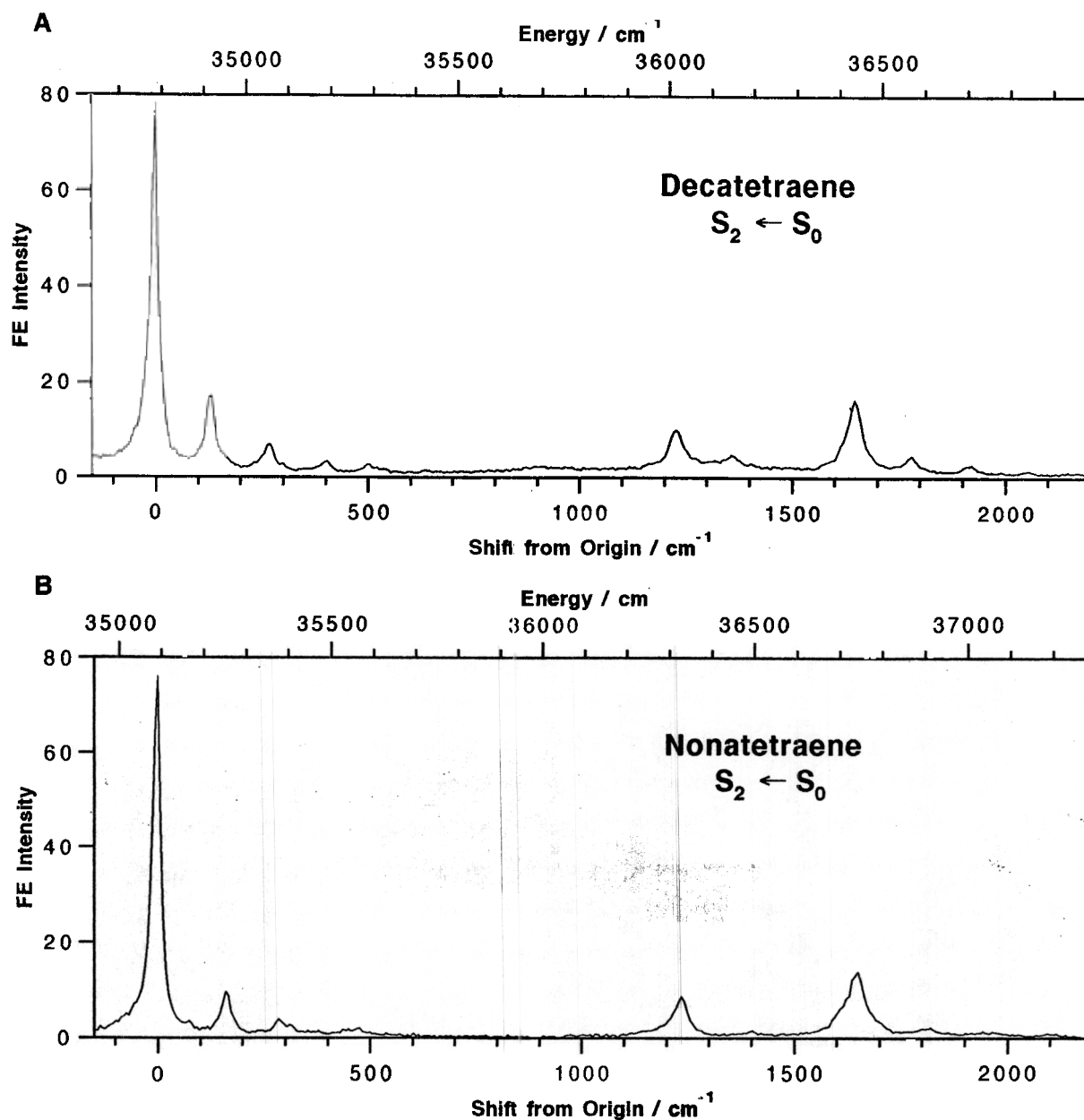


**Figure 6.** The  $S_2 \leftarrow S_0$  fluorescence excitation spectra of DT (a) and NT (b). The origins are at 34786 and 35091  $\text{cm}^{-1}$ , respectively. The  $\geq 21 \text{ cm}^{-1}$  Lorentzian linewidths are due to strong  $S_2 - S_1$  coupling which induces internal conversion on  $< 250 \text{ fs}$  timescale.

broad and intense peaks could be observed below the origin. This long lived decay and the associated structure is attributed to excitation to He:tetraene clusters and tetraene dimers and higher oligomers. The tetraene clusters can be observed with very high sensitivity because the fluorescence quantum yield of

tetraenes in the  $S_2$  state or in the isoenergetic highly vibrationally levels of the  $S_1$  state is very small for isolated molecules. Apparently the dissociation of tetraene clusters can compete with internal conversion to the  $S_0$  state. Dissociation of a cluster leaves the electronically excited tetraene with much lower internal energy and therefore higher fluorescence quantum yield than a monomer, for which this energy dissipation pathway is not available. By this mechanism a small concentration of clusters makes a significant contribution to the fluorescence excitation spectra in the region extending to  $\sim 1000\text{ cm}^{-1}$  below the  $S_2$  state origin.

The linewidths in the  $S_2$  state were found to be much broader than can be attributed to rotational structure or to methyl torsion. The line profiles were fitted to Lorentzian lineshapes with full-widths at half-maximum of  $\geq 21\text{ cm}^{-1}$  at the origin and  $> 40\text{ cm}^{-1}$  at CC stretches. There was no additional structure that could be resolved with the  $0.3\text{ cm}^{-1}$  laser resolution. Although Lorentzian lineshapes qualitatively described every peak, there were consistent deviations on most lines. These deviations could be of trivial nature such as the presence of a small amount of impurities such as *cis*-isomers tetraene complexes, and sequence bands from vibrationally excited molecules, which may be present due to the low He stagnation pressures; or more interestingly, the deviations may be caused by the  $S_2 - S_1$  interaction. The true cause for these deviations could not be determined because the  $S_2 \leftarrow S_0$  spectra of DT and NT are extremely sensitive to the experimental conditions. Due to these difficulties the reported linewidths represent an upper limit to the true Lorentzian linewidths of individual states. The observed linewidths imply that the  $S_2$  state internal conversion to the  $S_1$  state occurs on  $< 250\text{ fs}$  timescale.<sup>9</sup>

The increase in linewidths with excess energy in the  $S_2$  state implies an increase in nonradiative decay rates and a decrease in the emission quantum yields. The absorption spectrum of octatetraene has been observed in a molecular beam.<sup>14</sup> The comparison between the intensities of the CC stretches in the absorption spectrum of octatetraene and the fluorescence excitation spectra of DT and NT confirms that there is a gradual decrease in the fluorescence quantum yield with excess energy in the  $S_2$  states of tetraenes.

## 6. EMISSION SPECTRA FROM THE $S_1$ AND $S_2$ STATES OF TETRAENES

The observed  $S_2 \rightarrow S_0$  and  $S_1 \rightarrow S_0$  emission spectra measured by exciting the respective origins of decatetraene are shown in Fig. 5. The very different nature of the  $S_2 - S_0$  and  $S_1 - S_0$  optical transitions is very clearly demonstrated in these spectra. The  $S_2 \rightarrow S_0$  spectrum shows very simple structure which is dominated by CC stretches and weaker transitions due to the even quanta of in-plane bending. In the  $S_1 \rightarrow S_0$  spectrum there are many more states with significant transition moments. The overall envelope and the large Stokes shift are due to progressions in CC stretches, which have the largest Franck-Condon factors as discussed above. However, the comparison with the  $S_2 \rightarrow S_0$  spectrum shows that the most intense transitions are due to combinations bands of CC stretches and other low frequency modes. These low frequency modes can readily be assigned to the  $b_u$  symmetry in-plane bending modes which promote this symmetry forbidden transition.

## 7. CONCLUSIONS

Linear polyenes show several interesting trends in structure and reactivity as a function of conjugation length. Triene  $S_2$  and  $S_1$  states decay very rapidly by internal conversion to the  $S_0$  state. Only the *cis*-isomers have observable fluorescence in the  $S_1$  state, and even these decay by an activated nonradiative decay process with a  $< 200\text{ cm}^{-1}$  barrier. The spectra of *cis*-isomers show that the structures in the  $S_1$  state are nonplanar, and probably, that the methyl torsional angle changes between  $S_1$  and  $S_0$  states. Tetraenes are significantly more stable with respect to internal conversion in both  $S_2$  and  $S_1$  states. The structures appear to be planar, but in nonatetraene there is evidence for existence for two inequivalent minima on the  $S_1$  state surface, which arise from distortion in the in-plane bending

coordinate. This may be a common feature in longer polyenes. Both tetraenes show evidence for an activated nonradiative channel with a  $\sim 2000\text{ cm}^{-1}$  barrier, which is tentatively assigned to *cis-trans* isomerization. The  $S_2$  states of tetraenes are emissive and have well resolved structure with  $\geq 21\text{ cm}^{-1}$  Lorentzian linewidths. These linewidths are independent of methyl substitution. The homogeneous broadening in the  $S_2$  states of tetraenes is attributed to internal conversion to the  $S_1$  state in  $< 250\text{ fs}$ . The study of the structure and dynamics of short linear polyenes in free jet expansions provides important insights into the photochemistry of biologically and technologically important polyenes.

## 8. ACKNOWLEDGEMENTS

We are grateful to Royal Society/Japan Society for the Promotion of Science for support of AJB, the donors of the Petroleum Research Fund, administered by the American Chemical Society, and the DuPont Fund grant to Bowdoin College for partial support of research by RLC, B. Tounge for the preparation of octatriene, and I. Ohmine for invaluable discussions.

## 9. REFERENCES

1. B. S. Hudson, B. E. Kohler, K. Schulten, "Linear polyene electronic structures and potential Surfaces," in Excited States, ed. E. C. Lim, vol 6, pp 1-95, Academic Press, New York (1982).
2. G. Orlandi, F. Zerbetto, and M. Z. Zgierski, "Theoretical analysis of spectra of short polyenes," *Chem. Rev.* **91**, 867 (1991).
3. B. E. Kohler, "Electronic properties of linear polyenes," in Conjugated Polymers: The Novel Science and Technology of Conducting and Nonlinear Optically Active Materials, eds. J.L. Breads and R. Silby, pp 405- 434, Kluwer Press, Dodrecht (1991).
4. H. Petek, A. J. Bell, R. L. Christensen, and K. Yoshihara, "Fluorescence excitation spectra of the  $S_1$  states of isolated trienes," *J. Chem. Phys.* (in press).
5. H. Petek, A. J. Bell, K. Yoshihara, and R. L. Christensen, "Spectroscopic and dynamical studies of the  $S_1$  and  $S_2$  states of decatetraene in supersonic molecular beams," *J. Chem. Phys.* **95**, 4739 (1991).
6. W. G. Bouwman, A. C. Jones, D. Phillips, P. Thibodeau, C. Friel, and R. L. Christensen, "Fluorescence of gaseous tetraenes and pentaenes," *J. Phys. Chem.* **94**, 7429 (1990).
7. W. J. Buma, B. E. Kohler and K. Song, "Lowest energy excited singlet state of isolated *cis*-hexatriene," *J. Chem. Phys.*, **94**, 6367 (1991).
8. W. J. Buma, B. E. Kohler, K. Song, "Lowest energy excited singlet states of isomers of alkyl substituted hexatrienes," *J. Chem. Phys.* **94**, 4691 (1991).
9. H. Petek, A. J. Bell, R. L. Christensen, and K. Yoshihara, "Dynamical Study of Methyl Substituted Tetraenes in the  $S_1$  and  $S_2$  Electronically Excited States," (in preparation).
10. M. Aoyagi, I. Ohmine, and B. Kohler, "Frequency increase of the  $C = C a_g$  stretch mode of polyenes in the  $2^1A_g^-$  state: *Ab initio* MCSCF study of butadiene, hexatriene, and octatetraene," *J. Phys. Chem* **94**, 3922 (1990).
11. M. F. Granville, G. R. Holtom, B. E. Kohler, "High resolution one and two photon excitation spectra of *trans*, *trans*-1,3,5,7-octatetraene," *J. Chem. Phys.* **72**, 4671 (1980).
12. H. Yoshida, Y. Furukawa, and M. Tasumi, "Structural studies and vibrational analysis of stable and less stable conformers of 1,3,5-hexatriene based on *ab initio* calculations." *J. Mol. Struct.* **194**, 279 (1989).
13. B. E. Kohler, P. Mitra, and P. West, "Barriers in the excited  $2^1A_g$  state of *cis*, *trans*-octatetraene: General features and the excited state potential," *J. Chem. Phys.* **85**, 4436 (1986).
14. D. G. Leopold, V. Vaida, and M. F. Granville, "Direct absorption spectroscopy of jet-cooled polyenes. I. The  $^1B_u^+ \leftarrow ^1A_g^-$  transition of *trans*, *trans*-octatetraene," *J. Chem. Phys.* **81**, 4210 (1984).